Walter Steurer
Sofia Deloudi

SPRINGER SERIES IN MATERIALS SCIENCE 126

Crystallography of Quasicrystals

Concepts, Methods and Structures

Springer

Springer Series in
MATERIALS SCIENCE 126

Springer Series in
MATERIALS SCIENCE

The Springer Series in Materials Science covers the complete spectrum of materials physics, including fundamental principles, physical properties, materials theory and design. Recognizing the increasing importance of materials science in future device technologies, the book titles in this series reflect the state-of-the-art in understanding and controlling the structure and properties of all important classes of materials.

Walter Steurer
Sofia Deloudi

Crystallography of Quasicrystals

Concepts, Methods and Structures

With 177 Figures

Springer

Professor Dr. Walter Steurer
Dr. Sofia Deloudi
ETH Zürich, Department of Materials, Laboratory of Crystallography
Wolfgang-Pauli-Str. 10, 8093 Zürich, Switzerland
E-mail: steurer@mat.ethz.ch, deloudi@mat.ethz.ch

Springer Series in Materials Science ISSN 0933-033X
ISBN 978-3-642-01898-5 e-ISBN 978-3-642-01899-2
DOI 10.1007/978-3-642-01899-2
Springer Heidelberg Dordrecht London New York

Library of Congress Control Number: 2009929706

Preface

The quasicrystal community comprises mathematicians, physicists, chemists, materials scientists, and a handful of crystallographers. This diversity is reflected in more than 10,000 publications reporting 25 years of quasicrystal research. Always missing has been a monograph on the "Crystallography of Quasicrystals," a book presenting the main concepts, methods and structures in a self-consistent unified way; a book that translates the terminology and way of thinking of all these specialists from different fields into that of crystallographers, in order to look at detailed problems as well as at the big picture from a structural point of view.

Once Albert Einstein pointed out: "As far as the laws of mathematics refer to reality, they are not certain; as far as they are certain, they do not refer to reality." Accordingly, this book is aimed at bridging the gap between the ideal mathematical and physical constructs and the real quasicrystals of intricate complexity, and, last but not the least, providing a toolbox for tackling the structure analysis of real quasicrystals.

The book consists of three parts. The part "Concepts" treats the properties of tilings and coverings. If decorated by polyhedral clusters, these can be used as models for quasiperiodic structures. The higher-dimensional approach, central to the crystallography of quasicrystals, is also in the center of this part.

The part "Methods" discusses experimental techniques for the study of real quasicrystals as well as power and limits of methods for their structural analysis. What can we know about a quasicrystal structure and what do we want to know, why, and what for, this is the guideline.

The part "Structures" presents examples of quasicrystal structures, followed by a discussion of phase stability and transformations from a microscopical point of view. It ends with a chapter on soft quasicrystals and artificially fabricated macroscopic structures that can be used as photonic or phononic quasicrystals.

This book is intended for researchers in the field of quasicrystals and all scientists and graduate students who are interested in the crystallography of quasicrystals.

Zürich, *Walter Steurer*
June 2009 *Sofia Deloudi*

Contents

Acronyms

AC	Approximant crystal(s)
ADP	Atomic displacement parameter(s)
AET	Atomic environment type(s)
AFM	Atomic force microscopy
AT	Ammann tiling
bcc	Body-centered cubic
BZ	Brillouin Zone
CBED	Convergent-beam electron diffraction
ccp	Cubic close packed
CF	Charge flipping
CN	Coordination number
CS	Composite structure(s)
*d*D	*d*-dimensional
D_{m}	Mass density
D_{p}	Point density
fcc	Face-centered cubic
EXAFS	Extended X-ray absorption fine structure spectroscopy
FS	Fibonacci sequence
FT	Fourier transform
FWHM	Full width at half maximum
HAADF-STEM	High-angle annular dark-field scanning transmission electron microscopy
hcp	Hexagonal close packed
HRTEM	High-resolution transmission electron microscopy
HT	High temperature
IUCr	International union of crystallography
IMS	Incommensurately modulated structure(s)
K^{3D}	3D point group
LEED	Low-energy electron diffraction
LDE	Low-density elimination
LT	Low temperature

MC	Metacrystal(s)
ME	Mössbauer effect
MEM	Maximum-entropy method
nD	n-dimensional
ND	Neutron diffraction
NMR	Nuclear magnetic resonance
NS	Neutron scattering
PAS	Periodic average structure(s)
PC	Periodic crystal(s)
pdf	probability density function
PDF	Pair distribution function
PDS	Phason diffuse scattering
PF	Patterson function
PNC	Phononic crystal(s)
PT	Penrose tiling
PTC	Photonic crystal(s)
PNQC	Phononic quasicrystal(s)
PTQC	Photonic quasicrystal(s)
PV	Pisot-Vijayaraghavan
QC	Quasicrystal(s)
QG	Quiquandon-Gratias
SAED	Selected area electron diffraction
STM	Scanning tunneling microscopy
TDS	Thermal diffuse scattering
TM	Transition metal(s)
TEM	Transmission Electron microscopy
XRD	X-ray diffraction

Symbols

$F(\mathbf{H})$	Structure factor
$f_k\left(\lvert\mathbf{H}\rvert\right)$	Atomic scattering factor
F_n	Fibonacci number
G	Metric tensor of the direct lattice
G^*	Metric tensor of the reciprocal lattice
$\Gamma(R)$	Point group operation
$g_k\left(\mathbf{H}^{\perp}\right)$	Geometrical form factor
$\gcd(k,n)$	Greatest common divisor
$h_1\,h_2\ldots h_n$	Miller indices of a Bragg reflection (reciprocal lattice node) from the set of parallel lattice planes $(h_1\,h_2\ldots h_n)$
$(h_1\,h_2\ldots h_3)$	Miller indices denoting a plane (crystal face or single lattice plane)
M	Set of direct space vectors
M^*	Set of reciprocal space vectors
M_{F}^*	Set of Structure factor weighted reciprocal space vectors, i.e. Fourier spectrum
M_{I}^*	Set of intensity weighted reciprocal space vectors, i.e. diffraction pattern
λ_i	Eigenvalues
P_n	Pell number
$\rho(\mathbf{r})$	Electron density distribution function
S	Substitution and/or scaling matrix
σ	Substitution rule
Σ	nD Lattice
Σ^*	nD Reciprocal lattice
τ	Golden mean
$T_k\left(\mathbf{H}^{\parallel}\right)$	Temperature factor or atomic displacement factor
$[u_1\,u_2\ldots u_n]$	Indices denoting a direction
V	Vector space
$V^{\parallel}$	Parallel space (par-space)
$V^{\perp}$	Perpendicular space (perp-space)
W	Embedding matrix
w_n	nth word of a substitutional sequence

Part I

Concepts

In this first part of the book, the basic concepts and tools are presented for the description of quasicrystals and their structurally closely related periodic approximants. We will use both d-dimensional (dD) and n-dimensional (nD) approaches, where d is the dimension of the physical space and n that of the higher-dimensional embedding space ($n > d$).

In dD physical space, quasiperiodic structures can be described based on tilings or coverings. By tiling we mean a gapless packing of non-overlapping copies of a finite number of unit tiles. In analogy to a crystallographic lattice, such a tiling may be seen as a *quasilattice* with more than one unit cell of general shape. In a covering, one or more types of partially overlapping *covering clusters* fully cover a tiling or quasiperiodic pattern. In the nD description, dD quasiperiodic structures result from irrational physical-space cuts of appropriate periodic nD hypercrystal structures. Rational approximants can be obtained in the same way after shearing hypercrystal structures into the respective rational cut orientations.

In the nD approach, otherwise hidden structural correlations are revealed. For instance, the formation of diffraction patterns with Bragg reflections *and* 5-fold symmetry, causing so much controversy in the first time after the discovery of quasicrystals,[1] can be easily explained in this way. The nD approach also clearly identifies a particular kind of correlated atomic jumps (phason flips) as originating from phason modes, which are excitations already known from the study of incommensurately modulated structures. Despite the power and elegance of the nD approach, one has to keep in mind, however, that real quasicrystals are 3D objects and that their physical interactions take place in three dimensions, indeed.

What is a Crystal?

Before we define the term *quasicrystal* we should clarify what we mean by *crystal* and nD *(hyper)crystal*, in general. In the *International Tables for Crystallography, Vol A, chapter 8.1 Basic concepts*,[2] one will find the following:

> Crystals are finite real objects in physical space which may be idealized by infinite three-dimensional periodic crystal structures in point space. Three-dimensional periodicity means that there are translations among the symmetry operations of the object with the translation vectors spanning a three-dimensional space. Extending this concept of crystal structure to more general periodic objects and to n-dimensional space, one obtains the following definition:

[1] see, e.g., W. Steurer, S. Deloudi (2008): Fascinating Quasicrystals. Acta Crystallogr. A **64**, 1–11, and references therein.

[2] H. Wondratschek: Basic Concepts. In: International Tables for Crystallography, vol. A, Kluwer Academic Publisher, Dordrecht/Boston/London, pp. 720–740 (2002)

Definition: An object in n-dimensional point space E^n is called an n-dimensional crystallographic pattern or, for short, crystal pattern if among its symmetry operations

(i) there are n translations, the translation vectors $\mathbf{t}_1, \ldots, \mathbf{t}_n$ of which are linearly independent,

(ii) all translation vectors, except the zero vector $\mathbf{o}$, have a length of at least $d > 0$.

Condition (i) guarantees the n-dimensional periodicity and thus excludes subperiodic symmetries like layer groups, rod groups and frieze groups. Condition (ii) takes into account the finite size of atoms in actual crystals.

A crucial property of ideal, fully ordered crystals of any dimension is that they possess pure point Fourier spectra. This means that their diffraction patterns show Bragg reflections (Dirac δ-peaks) only, and no structural diffuse scattering. A real crystal can be described by comparing it with the model of an ideal crystal and by classifying the deviations from it. In the following, some terms are listed which are used for the description of real crystals or their idealized models:

Ideal crystal The counterpart to a real crystal. Infinite mathematical object with an idealized crystal structure; an ideal crystal can be ordered or disordered (disordered ideal crystal); if it is disordered, it is not periodic anymore, however, it has a periodic average structure.

Real crystal The counterpart to an ideal crystal. Really existing crystal which can be perfect or imperfect.

Perfect crystal Crystal in thermodynamic equilibrium, which can be ordered or disordered; the only defects possible are point defects such as thermal vacancies, impurities.

Imperfect crystal Crystal containing additionally defects that are not in thermodynamic equilibrium such as dislocations.

Nanocrystal Real crystal with dimensions on the scale of nanometers; due to the large surface area, its structure may fundamentally differ from that of larger crystals with the same composition and thermal history.

Metacrystal Crystal consisting of building units other than atoms (ions, molecules), such as photonic or phononic crystals.

What is a Quasicrystal?

One of the terms missing in the above list is *aperiodic crystal* which is used as hypernym for incommensurately modulated structures (IMS), composite crystals (CS), and quasicrystals QC. Although their structures lack dD translational periodicity, their Fourier spectra show Bragg peaks only. This property has been used by the *IUCr Ad-interim Commission on Aperiodic Crystals* to identify aperiodic crystals by their *essentially discrete diffraction diagram*.[3]

[3] *Ad interim Commission on Aperiodic Crystals*. Acta Crystallogr. A **48**, 928 (1992)

Consequently, dD translational periodicity is no more seen as a necessary condition for crystallinity. The reciprocal space definition of a crystal by its spectral properties can be much simpler than the one based on direct space. Additionally, it has the advantage of being directly accessible experimentally by diffraction methods.

However pragmatic this definition may be, it is also fuzzy. The term diffraction diagram refers to an experimentally obtained image, but does not take into account that the shapes of reflections depend on the kind of radiation used, the resolution and dynamic range of the detector as well as the quality and size of the crystal studied. A strongly absorbing, large, and irregularly shaped crystal of poor quality, for instance, would not at all give an essentially discrete diffraction diagram even for simple periodic structures.

Consequently, the concept of an aperiodic crystal has to refer to an ideal aperiodic crystal of infinite size and to its Fourier spectrum rather than to its diffraction image. A definition of the different types of aperiodic crystals in general and of quasicrystals in particular will be given in chapter 3.

How do we use the term *quasicrystal* in this book? By the term *quasicrystal* we denote real crystals with diffraction patterns showing *non-crystallographic symmetry*. This experiment-related reciprocal space definition of quasicrystals makes symmetry analysis simple and allows the application of tools that are well established in standard crystal structure analysis.

We clearly want to distinguish between quasicrystals (QC) in this meaning and the other kinds of aperiodic crystals with *crystallographic symmetry* such as incommensurately modulated structures (IMS) and composite structures (CS). In the mathematical meaning of the term quasiperiodicity, all three of them are quasiperiodic structures, which have some similarities in their higher-dimensional description. The main difference between a QC and an IMS is that an IMS can be described as modulation of a periodic crystal structure. If the modulation amplitude approaches zero, the periodic basic structure of the IMS is obtained. A CS, on the other hand, can be described as, sometimes mutually modulated, intergrowth of periodic structures. Such a direct one-to-one relationship to periodic structures is not possible in the case of QC with non-crystallographic symmetry.

Furthermore, for both IMS and CS, the orientational (rotational point) symmetry does not place any constraint on the irrational length scales involved. This is different for QC, where, for instance, the number $\tau = 2 \cos \pi/5$ is related to 5-fold rotational symmetry.

Finally, we do not use the terms *quasicrystal* and *quasiperiodic structure* synonymously. QC may have strictly quasiperiodic structures with *non-crystallographic symmetry* in an idealized description. However, their structure may also be quasiperiodic on average only; or, even only somehow related to quasiperiodicity. Strictly quasiperiodic structures must obey the closeness condition in the nD description, this may not be the case for the structure of real QC, which then would correspond to a kind of lock-in state.

Structural Complexity

Unary phases A: If, due to only isotropic interactions, each atom is equally densely surrounded by the other atoms in the first coordination shell, dense sphere packings are the consequence. Atomic environment types (AET) can either be cuboctahedra, such as in *fcc cF*4-Al, or disheptahedra, such as in *hcp hP*2-Mg, with the coordination number CN=12 in both cases. In case of anisotropic interactions (directional bonding, magnetic interactions, disproportionation under pressure, etc.), more complex structures can form such as *cI*58-Mn or *oC*84-Cs-III.[4] Anisotropic interactions, however, can also lead to the geometrically simplest possible structure, that of *cP*1-Po.[5]

Binary phases A–B: In a binary intermetallic compound A_xB_y, each atom has to be surrounded by at least some atoms of the other species in order to maximize the number of attractive interactions, otherwise the pure element phases would separate. Stoichiometry, atomic size ratios, directionality of atomic interactions, and the electronic band structure determine the respective AET. These may comprise several coordination shells and are usually called clusters.

The size of the unit cell of an intermetallic compound is determined by the most efficient packing of its constituting AET (clusters), which is that with the lowest free energy, of course. Consequently, the most efficient packing can be quite different for high- and low-temperature phases due to the entropical contributions of thermal vibrations and chemical disorder. The complexity of binary intermetallic compounds ranges between *cP*2-NiAl and *mC*7,448-Yb_2Cu_9.[6]

Ternary phases A-B-C: On the one hand, three different constituents give more flexibility in optimizing interactions. On the other hand, particularly in the case of repulsive interactions between two of the three atom types, it can get much more difficult to realize the most efficient packing. More different AET or clusters may be needed to create the optimum environments of A, B, and C. The complexity of ternary intermetallic compounds ranges between *hP*3-BaPtSb[7] and *cF*23,158-$Al_{55.4}Cu_{5.4}Ta_{39.1}$.[8]

---

[4] McMahon, M.I., Nelmes, R.J., Rekhi, S.: Complex Crystal Structure of Cesium-III. Phys. Rev. Lett. **87**, art. no. 255502 (2001)

[5] Legut, D., Friák, M., Šob, M.: Why is polonium simple cubic and so highly anisotropic? Phys. Rev.Lett. **99**, art. no. 016402 (2007)

[6] Černý, R., François, M., Yvon, K., Jaccard, D., Walker, E., Petříček, V., Císařová, I., Nissen, H.-U., Wessicken, R.: A single-crystal x-ray and HRTEM study of the heavy-fermion compound $YbCu_{4.5}$. J. Condens. Matter **8**, 4485–4493 (1996)

[7] Villars, P., Calvert, L. D.: Pearsons Handbook of Crystallographic Data for Intermetallic Phases (ASM, USA), Vols. 1–4 (1991)

[8] Weber, T., Dshemuchadse, J., Kobas, M., Conrad, M., Harbrecht, B., Steurer, W.: Large, larger, largest - a family of cluster-based tantalum-copper-aluminides with giant unit cells. Part A: Structure solution and refinement. Acta Crystallogr. B **65**, 308–317 (2009)

In case of quasicrystals, the number of different clusters in a particular compound is small, usually only one or two. Quasiperiodic long-range order mainly originates from their non-crystallographic symmetry together with their ability to overlap in a well-defined way with each other.

The question is, how complex are quasicrystals compared to periodic intermetallics? Are they more complex than the most complex periodic compounds, such as cF23,158-$Al_{55.4}Cu_{5.4}Ta_{39.1}$, built from much more different unit clusters than any QC?

Structural complexity is difficult to define. It is certainly not sufficient to just count the number of atoms per unit cell, what would be impossible for a quasicrystal anyway. For instance, the 192 atoms located on the general Wyckoff position in a cubic unit cell with space group symmetry $Fm\bar{3}m$, can be described just by the coordinates of a single atom, i.e. 3 parameters. For the same number of atoms in a triclinic unit cell and space group $P1$, 576 parameters would be needed. On the other hand, it is also not just the number of free parameters. A cubic structure with space group symmetry $Fm\bar{3}m$ and 4 atoms per unit cell needs three parameters, as well, but it seems to be much simpler. Particularly, because it is just the cubic closest packing.

One possibility for indicating the degree of complexity could be the number of different AET or the R-atlas. The R-atlas of a structure consists of all different atomic configurations within a circle of radius R. This may work for comparing (quasi)periodic structures with (quasi)periodic ones, but not for comparing periodic with quasiperiodic structures. In the latter case, one could compare, for instance, the R-atlases up to a maximum R, which is given by the dimensions of the unit cell.

Another possibility would be to compare the information needed to fully describe the one and the other structure or to grow it in the computer.
Complexity is reflected in

- broad distribution functions (histogramms) of atomic distances,
- large number of different AETs for each kind of atom,
- large number of independent parameters for the description of a structure,
- low symmetry.

Complexity results from

- unfavorable size ratios of atoms hindering geometrically optimum interactions,
- preference of coordinations (AET, clusters) hindering optimum packings (e.g. 5-fold symmetry),
- parameters that are close to optimum but not optimal (pseudosymmetry).

1

Tilings and Coverings

A packing is an arrangement of non-interpenetrable objects touching each other. The *horror vacui* of Mother Nature leads to the densest possible packings of structural units (atoms, ions, molecules, coordination polyhedra, atomic clusters, etc.) under constraints such as directional chemical bonding or charge balance. Of course, in the case of real crystals, the structural units are not hard spheres or rigid entities but usually show some flexibility. Consequently, the real packing density, i.e. the ratio of the volume filled by the atoms to the total volume, may differ considerably from that calculated for rigid spheres. For instance, the packing density $D_\mathrm{p} = \pi\sqrt{3}/16 = 0.34$ of the diamond structure is very low compared to $D_\mathrm{p} = \pi/\sqrt{18} = 0.74$ of the dense sphere packing. However, this low number does not reflect the high density and hardness of diamond, it just reflects the inappropriateness of the hard sphere model due to the tetrahedrally oriented, strong covalent bonds. Dense packing can be entropically disfavored at high temperatures. The *bcc* structure type, for instance, with $D_\mathrm{p} = \pi\sqrt{3}/8 = 0.68$, is very common for high-temperature (HT) phases due to its higher vibrational entropy compared to *hcp* or *ccp* structures.

If the packing density equals one, the objects fill space without gaps and voids and the packing can be described as tiling. nD periodic tilings can always be reduced to a packing of copies of a single unit cell, which corresponds to a nD parallelotope (parallelepiped in 3D, parallelogram in 2D). In case of quasiperiodic tilings at least two unit cells are needed.

Quasiperiodic tilings can be generated by different methods such as the (i) substitution method, (ii) tile assembling guided by matching rules, (iii) the higher-dimensional approach, and (iv) the generalized dual-grid method [3, 6]. We will discuss the first three methods.

Contrary to packings and tilings, coverings fill the space without gaps but with partial overlaps. There is always a one-to-one correspondence between coverings and tilings. Every covering can be represented by a (decorated) tiling. However, not every tiling can be represented by a covering based on a finite number of covering clusters. Usually, certain patches of tiles are taken for the construction of covering clusters.

In this chapter, we will discuss examples of basic tilings and coverings, which are crucial for the description and understanding of the quasicrystal structures known so far. Consequently, the focus will be on tilings with pentagonal, octagonal, decagonal, dodecagonal, and icosahedral diffraction symmetry. They all have in common that their scaling symmetries are related to quadratic irrationalities. This is also the case for the 1D Fibonacci sequence, which will also serve as an easily accessible and illustrative example for the different ways to generate and describe quasiperiodic tilings. The heptagonal (tetrakaidecagonal) tiling, which is based on cubic irrationalities, is discussed as an example of a different class of tilings. No QC are known yet with this symmetry, only approximants such as particular borides (see Sect. 8.1).

The reader who is generally interested in tilings is referred to the comprehensive book on *Tilings and Patterns* by Grünbaum and Shephard [9], which contains a wealth of tilings of all kinds. A few terms used for the description of tilings are explained in the following [19, 23, 34, 35].

Local isomorphism (LI) Two tilings are locally isomorphic if and only if *every* finite region contained in either tiling can also be found, in the same orientation, in the other. In other words, locally isomorphic tilings have the same R-atlases for all R, where the R-atlas of a tiling consists of all its tile patches of radius R. The LI class of a tiling is the set of all locally isomorphous tilings. Locally isomorphic structures have the same autocorrelation (Patterson) function, i.e. they are homometric. This means they also have the same diffraction pattern. Tilings, which are self-similar, have matching rules and an Ammann quasilattice are said to belong to the *Penrose local isomorphism* (PLI) class.

Orientational symmetry The tile edges are oriented along the set of star vectors defining the orientational (rotational) symmetry N. While there may be many points in regular tilings reflecting the orientational symmetry locally, there is usually no point of global symmetry. This is the case for exceptionally singular tilings. Therefore, the point-group symmetry of a tiling is better defined in reciprocal space. It is the symmetry of the structure factor (amplitudes and phases) weighted reciprocal (quasi)lattice. It can also be defined as the symmetry of the LI class.

Self-similarity There exists a mapping of the tiling onto itself, generating a tiling with larger tiles. In the case of a substitution tiling, this mapping is called *inflation* operation since the size of the tiles is distended. The inverse operation is *deflation* which shrinks the tiling in a way that each old tile of a given shape is decorated in the same way by a patch of the new smaller tiles. Self-similarity operations must respect matching rules. Sometimes the terms *inflation* (*deflation*) are used just in the opposite way referring to the increased (decreased) number of tiles generated.

Matching rules These constitute a construction rule forcing quasiperiodicity, which can be derived either from substitution (deflation) rules or

based on the nD approach. Matching rules can be coded either in the decoration of the tiles or in their shape. A tiling is said to admit *perfect* matching rules of radius R, if all tilings with the same R-atlas are locally isomorphic to it. A set of matching rules is said to be *strong*, if all tilings admitted are quasiperiodic, but not in a single LI class. *Weak* matching rules are the least restrictive ones which guarantee quasiperiodicity. They allow bounded departures from a perfect quasiperiodic tiling. The diffraction pattern will show diffuse scattering beside Bragg diffraction. Non-local matching rules need some global information on the tiling. They rather allow to check whether a tiling is quasiperiodic than to be used as a growth rule.

Ammann lines Tilings of the PLI class have the property that, if their unit tiles are properly decorated by line segments, these join together in the tiling and form sets of continuous lines (Ammann lines). According to the orientational symmetry, N sets of parallel, quasiperiodically spaced lines form, which are called Amman N-grid or Ammann quasilattice. Contrary to a periodic N grid with non-crystallographic symmetry, it has a finite number of Voronoi cell shapes.

Remark The explanations, definitions, and descriptions in the gray boxes are intended to give a simple and intuitive understanding of the concepts. Therefore, they are not always written in a mathematically rigorous style.

1.1 1D Substitutional Sequences

Besides several quasiperiodic sequences, examples of other kinds of non-periodic substitutional sequences will also be discussed, showing what they have in common and what clearly distinguishes them. The quasiperiodic sequences treated here are the Fibonacci sequence, which plays an important role in tilings with 5-fold rotational symmetry, and the Octonacci sequence, also known as Pell sequence, which is related to tilings with 8-fold symmetry.

The non-quasiperiodic sequences discussed here are the almost periodic squared Fibonacci sequence and the critical Thue–Morse sequence. The squared Fibonacci sequence has a fractal atomic surface and a pure point Fourier spectrum of infinite rank, while the Thue–Morse sequence shows a singular continuous spectrum. Both are mainly of interest for artificial structures such as photonic or phononic crystals. Finally, the properties of a randomized Fibonacci sequence will be shortly discussed.

1.1.1 Fibonacci Sequence (FS)

The Fibonacci sequence, a 1D quasiperiodic substitutional sequence (see, e.g., [26]), can be obtained by iterative application of the substitution rule $\sigma : \mathrm{L} \mapsto \mathrm{LS}, \mathrm{S} \mapsto \mathrm{L}$ to the two-letter alphabet {L, S}. The substitution rule can be alternatively written employing the substitution matrix S

$$\sigma : \begin{pmatrix} \mathrm{L} \\ \mathrm{S} \end{pmatrix} \mapsto \underbrace{\begin{pmatrix} 1 & 1 \\ 1 & 0 \end{pmatrix}}_{=\mathsf{S}} \begin{pmatrix} \mathrm{L} \\ \mathrm{S} \end{pmatrix} = \begin{pmatrix} \mathrm{LS} \\ \mathrm{L} \end{pmatrix}. \tag{1.1}$$

The substitution matrix does not give the order of the letters, just their relative frequencies in the resulting words w_n, which are finite strings of the two kinds of letters. Longer words can be created by multiple action of the substitution rule. Thus, $w_n = \sigma^n(\mathrm{L})$ means the word resulting from the n-th iteration of σ (L): $\mathrm{L} \mapsto \mathrm{LS}$. The action of the substitution rule is also called inflation operation as the number of letters is inflated by each step. The FS can as well be created by recursive concatenation of shorter words according to the concatenation rule $w_{n+2} = w_{n+1}w_n$. The generation of the first few words is shown in Table 1.1.

The frequencies $\nu_n^{\mathrm{L}} = F_{n+1}, \nu_n^{\mathrm{S}} = F_n$ of letters L, S in the word $w_n = \sigma^n(\mathrm{L})$, with $n \geq 1$, result from the $(n-1)$th power of the transposed substitution matrix to

$$\begin{pmatrix} \nu_n^{\mathrm{L}} \\ \nu_n^{\mathrm{S}} \end{pmatrix} = (\mathsf{S}^T)^{n-1} \begin{pmatrix} 1 \\ 1 \end{pmatrix}. \tag{1.2}$$

The Fibonacci numbers $F_{n+2} = F_{n+1} + F_n$, with $n \geq 0$ and $F_0 = 0, F_1 = 1$, form a series with $\lim_{n\to\infty} F_n/F_{n-1} = \tau = 1.618\ldots$, which is called the *golden ratio*. Arbitrary Fibonacci numbers can be calculated directly by Binet's formula

Table 1.1. Generation of words $w_n = \sigma^n(\mathrm{L})$ of the Fibonacci sequence by repeated action of the substitution rule $\sigma(\mathrm{L}) = \mathrm{LS}, \sigma(\mathrm{S}) = \mathrm{L}$. ν_n^{L} and ν_n^{S} denote the frequencies of L and S in the words w_n; F_n are the Fibonacci numbers

n	$w_{n+2} = w_{n+1}w_n$	ν_n^{L}	ν_n^{S}
0	L	1	0
1	LS	1	1
2	LSL	2	1
3	LSLLS	3	2
4	LSLLSLSL	5	3
5	LSLLSLSLLSLLS	8	5
6	$\underbrace{\mathrm{LSLLSLSLLSLLS}}_{w_5}\underbrace{\mathrm{LSLLSLSL}}_{w_4}$	13	8
$\vdots$	$\vdots$	$\vdots$	$\vdots$
n		F_{n+1}	F_n

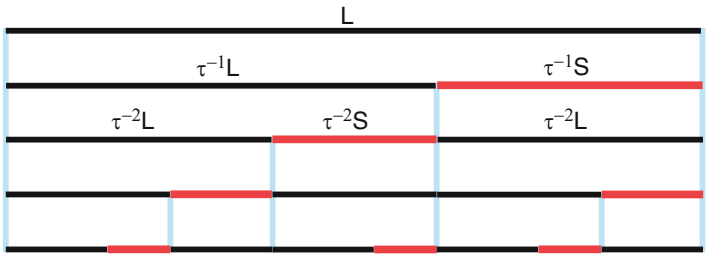

Fig. 1.1. Graphical representation of the substitution rule σ of the Fibonacci sequence. Rescaling by a factor $1/\tau$ at each step keeps the total length constant. Shown is a deflation of the line segment lengths corresponding to an inflation of letters

$$F_n = \frac{(1+\sqrt{5})^n - (1-\sqrt{5})^n}{2^n\sqrt{5}}. \tag{1.3}$$

The number τ If a line segment is divided in the *golden ratio*, then this *golden section* has the property that the larger subsegment is related to the smaller as the whole segment is related to the larger subsegment (Fig. 1.1). This way of creating harmonic proportions has been widely used in art and architecture for millenniums. The symbol τ is derived from the Greek noun $\tau o\mu\acute{\eta}$ which means cut, intersection. Alternatively, the symbol ϕ is used frequently. τ can be represented by the simplest possible continued fraction expansion

$$\tau = 1 + \frac{1}{1 + \frac{1}{1+\frac{1}{1+\ldots}}}. \tag{1.4}$$

Since it only contains the numeral one, it is the irrational number with the worst truncated continued fraction approximation. The convergents c_i are just ratios of two successive Fibonacci numbers

$$c_1 = 1, \quad c_2 = 1 + \frac{1}{1} = 2, \quad c_3 = 1 + \frac{1}{1+\frac{1}{1}} = \frac{3}{2}, \ldots, c_n = \frac{F_{n+1}}{F_n}. \tag{1.5}$$

This poor convergence is the reason that τ is sometimes called the "most irrational number." The strong irrationality may impede the lock-in of incommensurate (quasiperiodic) into commensurate (periodic) systems such as rational approximants.

The scaling properties of the FS can be derived from the eigenvalues λ_i of the substitution matrix S. For this purpose, the eigenvalue equation

$$\det|\mathsf{S} - \lambda\mathsf{I}| = 0, \tag{1.6}$$

with the unit matrix I, has to be solved. The evaluation of the determinant yields the characteristic polynomial

$$\lambda^2 - \lambda - 1 = 0 \tag{1.7}$$

with the eigenvalues $\lambda_1 = (1+\sqrt{5})/2 = 2\cos\pi/5 = 1.618\ldots = \tau$, $\lambda_2 = (1-\sqrt{5})/2 = -2\cos 2\pi/5 = -0.618\ldots = 1-\tau = -1/\tau$ and the eigenvectors

$$\mathbf{v}_1 = \begin{pmatrix} \tau \\ 1 \end{pmatrix}, \quad \mathbf{v}_2 = \begin{pmatrix} -1/\tau \\ 1 \end{pmatrix}. \tag{1.8}$$

We can now explicitly write the eigenvalue equation $\mathsf{S}\mathbf{v}_i = \lambda_i \mathbf{v}_i$ for the first eigenvalue, for instance,

$$\begin{pmatrix} 1 & 1 \\ 1 & 0 \end{pmatrix} \begin{pmatrix} \tau \\ 1 \end{pmatrix} = \begin{pmatrix} \tau+1 \\ \tau \end{pmatrix} = \tau \begin{pmatrix} \tau \\ 1 \end{pmatrix}. \tag{1.9}$$

If we assign long and short line segments, respectively, to the letters L and S we get the 1D Fibonacci tiling (Fig. 1.1). Relating the eigenvector $\begin{pmatrix} \tau \\ 1 \end{pmatrix}$ to $\begin{pmatrix} \mathrm{L} \\ \mathrm{S} \end{pmatrix}$ shows that an infinite Fibonacci tiling $s(\mathbf{r})$ is invariant under scaling with the eigenvalue τ, $s(\tau\mathbf{r}) = s(\mathbf{r})$.

The scaling operation maps each tiling vector $\mathbf{r}$ to an already existing tiling vector $\tau\mathbf{r}$. Consequently, the ratio of patches of the Fibonacci tiling, which correspond to words w_n and w_{n+1} created by successive application of the substitution matrix S, is given by the ratio of the eigenvector components

$$\frac{w_{n+1}}{w_n} = \frac{\mathrm{L}}{\mathrm{S}} = \frac{\mathrm{LS}}{\mathrm{L}} = \frac{\mathrm{LSL}}{\mathrm{LS}} = \frac{\mathrm{LSLLS}}{\mathrm{LSL}} = \cdots = \frac{\tau}{1}. \tag{1.10}$$

The length of a word $\ell(w_n)$ can be easily calculated to $\ell(w_n) = \tau^n \mathrm{L}$. The mean vertex distance, d_{av}, results to

$$d_{\mathrm{av}} = \lim_{n\to\infty} \frac{F_{n+1}\mathrm{L} + F_n\mathrm{S}}{F_{n+1}+F_n} = \left\{ \frac{F_{n+1}}{F_{n+2}}\tau + \frac{F_n}{F_{n+2}} \right\} \mathrm{S} = (3-\tau)\mathrm{S}, \tag{1.11}$$

yielding a vertex point density $D_{\mathrm{p}} = 1/d_{\mathrm{av}}$. $d_{\mathrm{av}} = a_{\mathrm{PAS}}$ is also the period of the periodic average structure (PAS) of the FS (see section 3.3). The total length of the Fibonacci tiling for n line segments reads, in units of S,

$$x_n = (n+1)(3-\tau) - 1 - \frac{1}{\tau}\left\{ \left[\frac{n+1}{\tau} \right] \mod 1 \right\}. \tag{1.12}$$

Periodic lattices scale with integer factors, thus the eigenvalues are integers. In case of quasiperiodic "lattices" (*quasilattices*), the eigenvalues are *algebraic numbers* (*Pisot numbers*), which have the *Pisot–Vijayaraghavan (PV) property*:

$$\lambda_1 > 1, \quad |\lambda_i| < 1 \quad \forall i > 1. \tag{1.13}$$

Thus, a Pisot number is a real algebraic number larger than one and its conjugates have an absolute value less than one. Tilings satisfy the PV property if they have point Fourier spectra. The PV property connected to this is that the n-th power of a Pisot number approaches integers as n approaches infinity. The PV property is a necessary condition for a pure point Fourier spectrum, however, it is not sufficient. The Thue–Morse sequence, for instance, has the PV property, but it has a singular continuous Fourier spectrum (see Sect. 1.1.4).

1.1.2 Octonacci Sequence

The Octonacci sequence, in mathematics better known as Pell sequence, describes the sequence of spacings of the Ammann quasilattice (8-grid) of the octagonal Ammann–Beenker tiling (see Sect. 1.2.5). The name Octonacci is composed from "Octo-" for octagonal and "-acci" from the Fibonacci sequence. It can be generated in analogy to the Fibonacci sequence by a substitution rule $\sigma : \mathrm{L} \mapsto \mathrm{LLS}, \mathrm{S} \mapsto \mathrm{L}$ to the two-letter alphabet {L, S} [42]. It can also be created by recursive concatenation of shorter words according to the concatenation rule $w_{n+2} = w_{n+1}w_{n+1}w_n$. The generation of the first few words is shown in Table 1.2. The substitution matrix S reads

$$\sigma : \begin{pmatrix} \mathrm{L} \\ \mathrm{S} \end{pmatrix} \mapsto \underbrace{\begin{pmatrix} 2 & 1 \\ 1 & 0 \end{pmatrix}}_{=\mathsf{S}} \begin{pmatrix} \mathrm{L} \\ \mathrm{S} \end{pmatrix} = \begin{pmatrix} \mathrm{LLS} \\ \mathrm{L} \end{pmatrix}. \tag{1.14}$$

The evaluation of the determinant of the eigenvalue equation yields the characteristic polynomial

$$\lambda^2 - 2\lambda - 1 = 0 \tag{1.15}$$

Table 1.2. Generation of words $w_n = \sigma^n(\mathrm{S})$ of the Octonacci sequence by repeated action of the substitution rule $\sigma(\mathrm{L}) = \mathrm{LLS}$, $\sigma(\mathrm{S}) = \mathrm{L}$. ν_n^{L} and ν_n^{S} denote the frequencies of L and S, f_n are the Pell numbers

n	$w_{n+2} = w_{n+1}w_{n+1}w_n$	ν_n^{L}	ν_n^{S}	$\nu_n^{\mathrm{L}} + \nu_n^{\mathrm{S}}$
0	S	0	1	1
1	L	1	0	1
2	LLS	2	1	3
3	LLSLLSL	5	2	7
4	LLSLLSLLLSLLSLLLS	12	5	17
5	$\underbrace{\mathrm{LLSLLSLLLSLLSLLLS}}_{w_4}\underbrace{\mathrm{LLSLLSLLLSLLSLLLS}}_{w_4}\underbrace{\mathrm{LLSLLSL}}_{w_3}$	29	12	41
⋮	⋮	⋮	⋮	
n		f_n	$g_n - f_n$	g_n

with the eigenvalues $\lambda_1 = 1+\sqrt{2} = (2+\sqrt{8})/2 = 2.41421\ldots = \omega$, $\lambda_2 = 1-\sqrt{2} = -0.41421\ldots$, which satisfy the PV property. The eigenvalue ω can be represented by the continued fraction expansion

$$\omega = 2 + \frac{1}{2+\frac{1}{2+\frac{1}{2+\ldots}}}. \tag{1.16}$$

The frequencies $\nu_n^{\mathrm{L}} = f_n, \nu_n^{\mathrm{S}} = g_n - f_n$ of letters L, S in the word $w_n = \sigma^n(\mathrm{S})$, with $n \geq 1$, result to

$$\begin{pmatrix} \nu_n^{\mathrm{L}} + \nu_n^{\mathrm{S}} \\ \nu_n^{\mathrm{L}} - \nu_n^{\mathrm{S}} \end{pmatrix} = (\mathsf{S}^T)^{n-1} \begin{pmatrix} 1 \\ 1 \end{pmatrix}. \tag{1.17}$$

The Pell numbers $f_{n+2} = 2f_{n+1} + f_n$, with $n \geq 0$ and $f_0 = 0$ and $f_1 = 1$, form a series with $\lim_{n\to\infty} f_{n+1}/f_n = 1+\sqrt{2} = 2.41421\ldots$, which is called the *silver ratio* or *silver mean*. They can be calculated as well by the following equation

$$f_n = \frac{\omega^n - \omega^{-n}}{\omega - \omega^{-1}} \tag{1.18}$$

The 2D analogue to the Octonacci sequence, a rectangular quasiperiodic 2-grid, can be constructed from the Euclidean product of two tilings that are each based on the Octonacci sequence. If only even or only odd vertices are connected by diagonal bonds then the so called Labyrinth tilings L_m and their duals L_m^*, respectively, result [42].

1.1.3 Squared Fibonacci Sequence

By squaring the substitution matrix S of the Fibonacci sequence, the squared FS can be obtained

$$\sigma : \begin{pmatrix} \mathrm{L} \\ \mathrm{S} \end{pmatrix} \mapsto \underbrace{\begin{pmatrix} 2 & 1 \\ 1 & 1 \end{pmatrix}}_{=\mathsf{S}^2} \begin{pmatrix} \mathrm{L} \\ \mathrm{S} \end{pmatrix} = \begin{pmatrix} \mathrm{LLS} \\ \mathrm{SL} \end{pmatrix}. \tag{1.19}$$

This operation corresponds to the substitution rule $\sigma : \mathrm{L} \mapsto \mathrm{LLS}, \mathrm{S} \mapsto \mathrm{SL}$ applied to the two-letter alphabet {L, S}.

The scaling properties of the squared FS can be derived from the eigenvalues λ_i of the substitution matrix S^2. For this purpose, the eigenvalue equation

$$\det|\mathsf{S}^2 - \lambda\mathsf{I}| = 0, \tag{1.20}$$

with the unit matrix I, has to be solved. The evaluation of the determinant yields the characteristic polynomial

$$\lambda^2 - 3\lambda + 1 = 0 \tag{1.21}$$

with the eigenvalues $\lambda_1 = \tau^2$, $\lambda_2 = 1/\tau^2 = 2-\tau$, which satisfy the PV property, and the same eigenvectors as for the FS. The generation of the first few words is shown in Table 1.3.

Table 1.3. Generation of words $w_n = \sigma^n(\mathrm{L})$ of the squared Fibonacci sequence by repeated action of the substitution rule $\sigma(\mathrm{L}) = \mathrm{LLS}$, $\sigma(\mathrm{S}) = \mathrm{SL}$ or by concatenation. ν_n^{L} and ν_n^{S} denote the frequencies of L and S in the words w_n, F_n are the Fibonacci numbers

n	$w_n = w_{n-1}w_{n-1}\overline{w}_{n-1}$, $\overline{w}_n = \overline{w}_{n-1}w_{n-1}$ with $w_0 = \mathrm{L}$ and $\overline{w}_0 = \mathrm{S}$	ν_n^{L}	ν_n^{S}
0	L	1	0
1	LLS	2	1
2	LLSLLSSL	5	3
3	LLSLLSSLLLSLLSSLSLLLS	13	8
4	$\underbrace{\mathrm{LLSLLSSLLLSLLSSLSLLLS}}_{w_3}\underbrace{\mathrm{LLSLLSSLLLSLLSSLSLLLS}}_{w_3}\underbrace{\mathrm{SLLLSLLSLLSSL}}_{\overline{w}_3}$	34	21
⋮	⋮	⋮	⋮
n		F_{2n+1}	F_{2n}

Table 1.4. Generation of words $w_n = \sigma^n(\mathrm{A})$ of the Thue–Morse sequence by repeated action of the substitution rule $\sigma(\mathrm{A}) = \mathrm{AB}$, $\sigma(\mathrm{B}) = \mathrm{BA}$ or by concatenation

n	$w_n = w_{n-1}\overline{w}_{n-1}$, $\overline{w}_n = \overline{w}_{n-1}w_{n-1}$ with $w_0 = \mathrm{A}$ and $\overline{w}_0 = \mathrm{B}$
0	A
1	AB
2	ABBA
3	ABBABAAB
4	ABBABAABBAABABBA
5	$\underbrace{\mathrm{ABBABAABBAABABBA}}_{w_4}\underbrace{\mathrm{BAABABBAABBABAAB}}_{\overline{w}_4}$
⋮	⋮

1.1.4 Thue–Morse Sequence

The (Prouhet-)Thue–Morse sequence results from the multiple application of the substitution rule $\sigma : \mathrm{A} \mapsto \mathrm{AB}, \mathrm{B} \mapsto \mathrm{BA}$ to the two-letter alphabet $\{\mathrm{A}, \mathrm{B}\}$. The substitution rule can be alternatively written employing the substitution matrix S

$$\sigma : \begin{pmatrix} \mathrm{A} \\ \mathrm{B} \end{pmatrix} \mapsto \underbrace{\begin{pmatrix} 1 & 1 \\ 1 & 1 \end{pmatrix}}_{=\mathsf{S}} \begin{pmatrix} \mathrm{A} \\ \mathrm{B} \end{pmatrix} = \begin{pmatrix} \mathrm{AB} \\ \mathrm{BA} \end{pmatrix}. \tag{1.22}$$

The frequencies in the sequence of the letters A and B are equal. The length of the sequence after the n-th iteration is 2^n. The Thue–Morse sequence can also be generated by concatenation: $w_{n+1} = w_n\overline{w}_n$, $\overline{w}_{n+1} = \overline{w}_n w_n$ with $w_0 = \mathrm{A}$ and $\overline{w}_0 = \mathrm{B}$ (Table 1.4).

The characteristic polynomial $\lambda^2 - 2\lambda = 0$ leads to the eigenvalues $\lambda_1 = 2$ and $\lambda_2 = 0$. Although these numbers show the PV property, the Fourier spectrum of the TMS can be singular continuous without any Bragg peaks. If we assign intervals of a given length to the letters A and B, then every other vertex belongs to a periodic substructure of period A+B. This is also the size of the unit cell of the PAS, which contains two further vertices at distances A and B, respectively, from its origin. All vertices of the PAS are equally weighted. The Bragg peaks, which would result from the PAS, are destroyed for special values of A and B by the special order of the Thue–Morse sequence leading to a singular continuous Fourier spectrum. The broad peaks split into more and more peaks if the resolution is increased. In the generic case, however, a Fourier module exists beside the singular continuous spectrum. Depending on the decoration, the Thue–Morse sequence will show Bragg peaks besides the singular continuous spectrum (see Fig. 6.2).

1.1.5 1D Random Sequences

It is not possible to say much more about general 1D random sequences than that their Fourier spectra will be absolutely continuous. However, depending on the parameters (number of prototiles, frequencies, correlations), the spectra can show rather narrow peaks for particular reciprocal lattice vectors. General formulas have been derived for different cases of 1D random sequences [15].

The diffraction pattern of a FS, decorated with Al atoms and randomized by a large number of phason flips, is shown in Fig. 1.2. Although the Fourier spectrum of such a random sequence is absolutely continuous, it is peaked for reciprocal space vectors of the type m/L and n/S with $m \approx n\tau$, with m and n two successive Fibonacci numbers.

The continuous diffuse background under the peaked spectrum of the randomized FS can be described by the relation $I_{\text{diff}} \sim f(h)[1 - \cos(2\pi h(L - S)]$ ($f_{\text{Al}}(h)$ is the atomic form factor of Al, L, and S are the long and short interatomic distances in the Al decorated FS).

1.2 2D Tilings

The symmetry of periodic tilings, point group and plane group (2D space group), can be given in a straightforward way (see, e.g., Table 1.7). In case of general quasiperiodic tilings, there is no 2D space or point group symmetry at all. Some tilings show scaling symmetry. In case of singular tilings, there is just one point of global point group symmetry other than 1. The orientational order of equivalent tile edges ("bond-orientational order"), however, is clearly defined and can be used as one parameter for the classification of tilings. This means, one takes one type of tile edge, which may be arrowed or not, in all orientations occurring in the tiling and forms a star. The point symmetry group of that star is then taken for classifying the symmetry of the tiling.

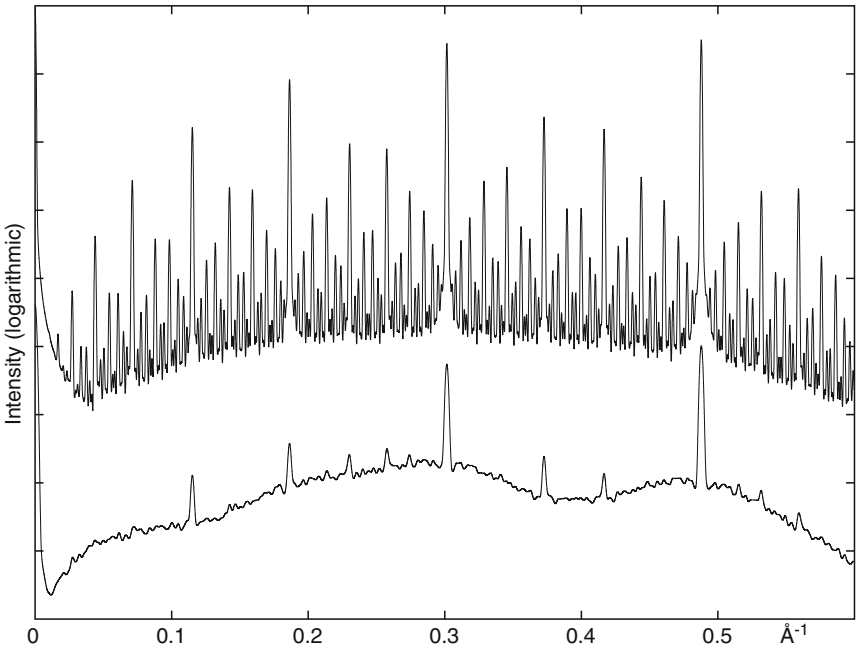

Fig. 1.2. Diffraction patterns of a Fibonacci sequence before (*top*) and after (*bottom*) partial randomization ($\approx$ 25% of all tiles have been flipped). The vertices of the Fibonacci sequence are decorated by Al atoms with the short distance S = 2.4 Å; the diffraction patterns have been convoluted with a Gaussian with FWHM = 0.001 Å^{-1} to simulate realistic experimental resolution (courtesy of Th. Weber)

Table 1.5. Point groups of 2D quasiperiodic structures (tilings) (based on [13]). Besides the general case with n-fold rotational symmetry, a few practically relevant special cases are given. k denotes the order of the group

Point group type k	Conditions	$n=5$	$n=7$	$n=8$	$n=10$	$n=12$	$n=14$
nmm	$2n$ n even			$8mm$	$10mm$	$12mm$	$14mm$
nm	$2n$ n odd	$5m$	$7m$				
n	n	5	7	8	10	12	14

This is related to the autocorrelation (Patterson) function. In Table 1.5, the possible point symmetry groups of 2D quasiperiodic structures (tilings) are given.

The general space group symmetries possible for 2D quasiperiodic structures with rotational symmetry $n \leq 15$ are listed in Table 1.6.

By taking the symmetry of the Patterson function for the tiling symmetry, it is not possible to distinguish between centrosymmetric and non-centrosymmetric tilings. This means that in the case of 2D tilings only

Table 1.6. Space groups of 2D quasiperiodic structures (tilings) (based on [32]). Besides the general case with n-fold rotational symmetry, a few practically relevant special cases are given. The lattice symmetry is $2n$ for n odd

Point group	Conditions	$n=5$	$n=7$	$n=8$	$n=10$	$n=12$	$n=14$
nmm	n even			$p8mm$	$p10mm$	$p12mm$	$p14mm$
	$n=2^p$			$p8gm$			
$nm1$	n odd	$5m1$	$7m1$				
$n1m$	n odd	$51m$	$71m$				
n		$p5$	$p7$	$p8$	$p10$	$p12$	$p14$

even rotational symmetries could be discriminated, both pentagonal and decagonal tilings have decagonal Patterson symmetry, for instance. The same is true for the Laue symmetry, which is the symmetry of the intensity weighted reciprocal space, i.e. of the Bragg intensity distribution.

The symmetry can also be defined for the local isomorphism (LI) class of a tiling. Then a tiling is said to admit a certain point symmetry, if this symmetry maps the tiling onto another tiling in the same LI class. The transformed tiling cannot be distinguished from the original one by any local means, since tilings of the same LI class are locally indistinguishable from each other. In this sense, the concept of point symmetry differs for quasiperiodic structures from periodic ones. The point group of a tiling here is the point group of its LI class. For a periodic tiling, the LI class consists of only one element, and the definition of point symmetry reduces to the usual one.

Perhaps the best approach is based on the symmetry of the structure-factor-weighted reciprocal lattice, which even allows to derive a kind of space group symmetry. The full equivalence of such a Fourier space approach to a derivation of space groups in direct space has been demonstrated for periodic structures by [5] and applied to quasiperiodic structures by [32]. This kind of space group symmetry corresponds to that which can be obtained from the higher-dimensional approach (see Chap. 3).

1.2.1 Archimedean Tilings

The Archimedean tilings, which are all periodic, have been derived by Kepler in analogy to the Archimedean solids (see Sect. 2.1). Three of them are regular, i.e. consist of congruent regular polygons and show only one type of vertex configuration. The regular tilings are the triangle tiling 3^6, the square tiling 4^4 and the hexagon tiling 6^3. A vertex configuration n^m is defined by the kind of polygons along a circuit around a vertex. For instance, 6^3 means that at a vertex 3 hexagons meet.

The eight semiregular tilings are uniform, i.e. have only one type of vertex (vertex transitive), and consist of two or more regular polygons as tiles.

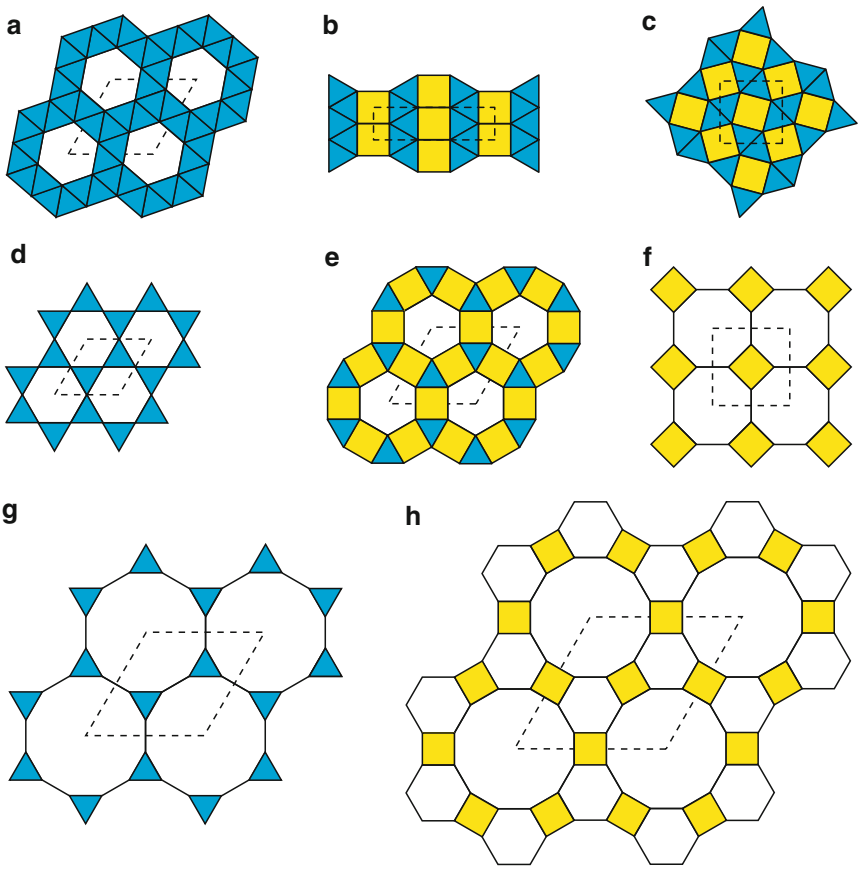

Fig. 1.3. The eight semiregular Archimedean tilings: (**a**) Snub hexagonal tiling $3^4.6$, (**b**) elongated triangular tiling $3^3.4^2$, (**c**) snub square tiling $3^2.4.3.4$, (**d**) trihexagonal tiling 3.6.3.6, (**e**) small rhombitrihexagonal tiling 3.4.6.4, (**f**) truncated square tiling 4.8^2, (**g**) truncated hexagonal tiling 3.12^2, and (**h**) great rhombitrihexagonal tiling 4.6.12. The unit cells are outlined by dashed lines

The Archimedean tilings are discussed here since they are quite common in structures of intermetallic phases and soft QC approximants. Particularly interesting for QC approximants are the tilings 4.8^2 with octagonal tiles, and 3.12 and 4.6.12, which contain dodecagonal tiles. Some characteristic data of the semiregular tilings that are depicted in Fig. 1.3 are listed in Table 1.7.

1.2.2 Square Fibonacci Tiling

The square Fibonacci tiling is a simple example of a 2D quasiperiodic tiling with crystallographic point symmetry ($4mm$) [24]. It can be generated, for instance, by superposition of two Fibonacci line grids, which are orthogonal

Table 1.7. Characteristic data for the eight semiregular Archimedean tilings. The number of vertices n_V per unit cell is given; the density is calculated for a close packing of equal circles at the vertices. In the second lines, the lattice parameter a is given for a tile edge length of 1 and the Wyckoff positions occupied are listed [28]

Name	Vertex Configuration	n_V	Plane Group a	Density Wyckoff position
Snub hexagonal tiling[a]	$3^4.6$	6	$p6$ $a=\sqrt{7}$	$\pi\sqrt{3}/7=0.7773$ $6(d)\ x=3/7, y=1/7$
Elongated triangular tiling	$3^3.4^2$	4	$c2mm$ $a=1$ $b=2+\sqrt{3}$	$\pi/(2+\sqrt{3})=0.8418$ $4(e)\ y=(1+\sqrt{3})/(4+2\sqrt{3})$
Snub square tiling	$3^2.4.3.4$	4	$p4gm$ $a=(2+\sqrt{3})^{1/2}$	$\pi/(2+\sqrt{3})=0.8418$ $4(c)\ x=1--1/4$ $[(2-\sqrt{3})(2+\sqrt{3})]^{1/2}$
Trihexagonal tiling[b]	3.6.3.6	3	$p6mm$ $a=2$	$\pi\sqrt{3}/8=0.6802$ $3(c)$
Small rhombitri-hexagonal tiling	3.4.6.4	6	$p6mm$ $a=1+\sqrt{3}$	$\pi\sqrt{3}/(4+2\sqrt{3})=0.7290$ $6(e)\ x=1/(3+\sqrt{3})$
Truncated square tiling	4.8^2	4	$p4mm$ $a=1+\sqrt{2}$	$\pi/(3+2\sqrt{2})=0.5390$ $4(e)\ x=1/(2+2\sqrt{2})$
Truncated hexagonal tiling	3.12^2	6	$p6mm$ $a=2+\sqrt{2}$	$\pi\sqrt{3}/(7+4\sqrt{3})=0.3907$ $6(e)\ x=(1-1/\sqrt{3})$
Great rhombitri-hexagonal tiling	4.6.12	12	$p6mm$ $a=3+\sqrt{3}$	$\pi/(3+2\sqrt{3})=0.4860$ $12(f)\ x=1/(3\sqrt{3}+3),$ $y=x+1/3$

[a] Two enantiomorphs
[b] Kagome net; quasiregular tiling because all edges are shared by equal polygons

to each other (Fig. 1.4). The substitution rule, also depicted in Fig. 1.4, can be written employing the substitution matrix S

$$\mathsf{S}=\begin{pmatrix}1&1&1\\1&0&0\\2&0&1\end{pmatrix}, \tag{1.23}$$

with the characteristic polynom $-x^3+2x^2+2x-1=-(1+x)(1-3x+x^2)$ and the eigenvalues $\lambda_1=\tau^2$ and $\lambda_2=\tau^{-2}$ for the irreducible component $(1-3x+x^2)$. Therefore, the PV property is fulfilled. The tile frequencies are τ^{-2} for the large squares, τ^{-4} for the small squares and $2\tau^{-3}$ for the rectangles (independent from their orientation).

The square Fibonacci tiling is quasiperiodic, if based on prototiles of different sizes. In case the FS results from a quasiperiodic distribution of two types of atoms, or atoms and vacancies on a periodic lattice, then one periodic direction can result. In the example shown in Fig. 1.5, a square lattice is decorated

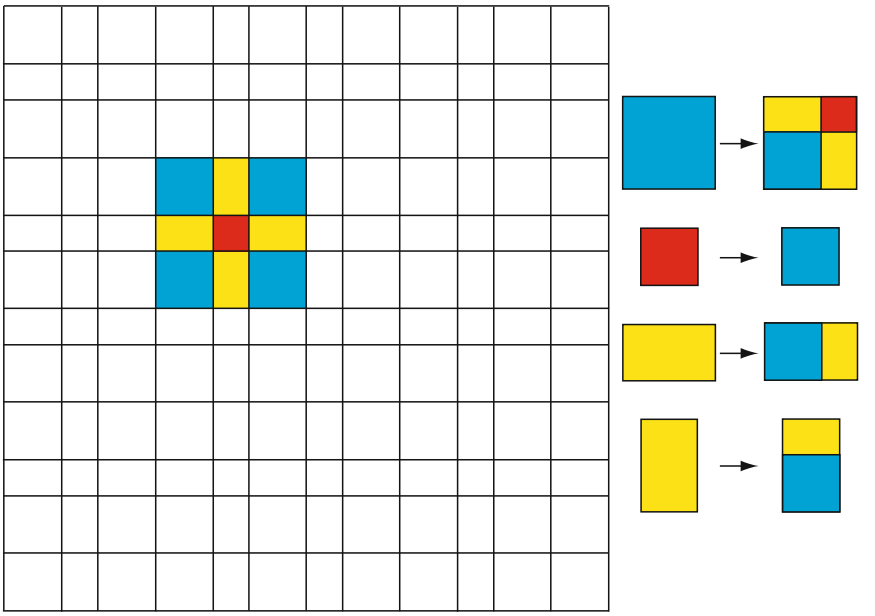

Fig. 1.4. The square Fibonacci tiling generated by superposition of two, to each other orthogonal, Fibonacci line grids. The minimum covering cluster is marked in the tiling, the inflation rule is shown at right

by full circles (L) and vacancies (S) like a FS in two orthogonal directions and with one mirror line along one diagonal. One of the two diagonal directions of the underlying lattice then results to be periodic. This pattern has the property that vacancies are never closer to each other than one square diagonal and that they are fully surrounded by the filled circles with the distance of one square edge.

Analogously, the 3D cube Fibonacci tiling can be created, which may be of interest for vacancy ordered structures.

1.2.3 Penrose Tiling (PT)

The Penrose tiling was discovered by Roger Penrose [30] and popularized by Martin Gardner in the popular scientific journal *Scientific American* [8]. There are several versions of the PT presented in the book *Tilings and Patterns* by Grünbaum and Shephard [9]: a pentagon based tiling (P1), a kite and dart version of it (P2) and a rhomb tiling (P3). All three of them are mutually locally derivable and belong to the Penrose local isomorphism (PLI) class. According to its reciprocal space symmetry, the PT is a decagonal quasiperiodic tiling. The PLI class tilings possess matching rules that force quasiperiodicity. If the matching rules are relaxed other tilings become possible, which may be quasiperiodic, periodic, or all kinds of non-periodic up to

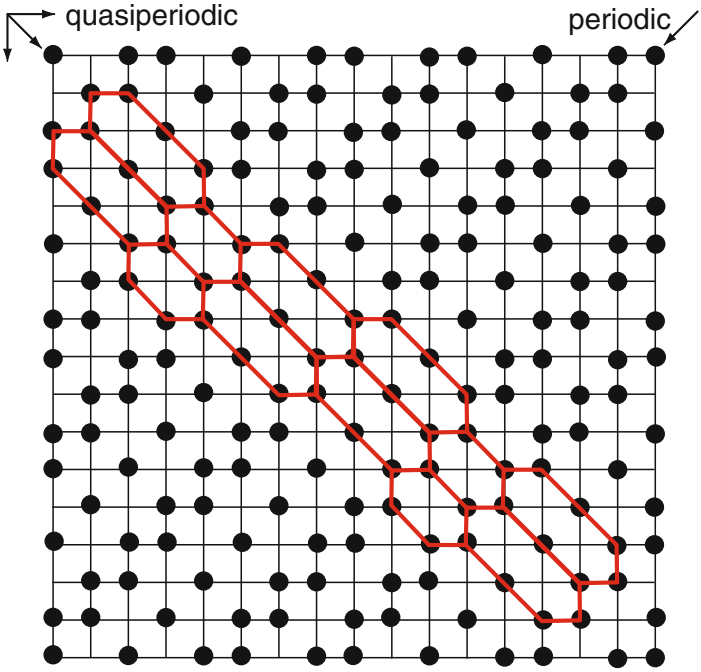

Fig. 1.5. Substitutional square Fibonacci tiling. The vertices of a square lattice are either occupied (*full circles*) or unoccupied. Along the horizontal and vertical axes as well as along one diagonal the substitutional sequence (distances between occupied vertices) is the Fibonacci sequence. Along the other diagonal, the pattern is periodic

fully random. The binary tiling will be discussed as an example, which may have some importance for the description of real quasicrystals.

1.2.3.1 Rhomb Penrose Tiling

The rhomb PT [29, 30] can be constructed from two unit tiles: a skinny (acute angle $\alpha = \pi/5$) and a fat rhomb (acute angle $\alpha = 2\pi/5$) with equal edge lengths a_r and areas $a_r^2 \sin \pi/5$ and $a_r^2 \sin 2\pi/5$, respectively. Their areas and frequencies in the PT are both in the ratio $1 : \tau$. The construction has to obey matching rules, which can be derived from the scaling properties of the PT (Fig. 1.6). The local matching rules are perfect, that means that they force quasiperiodicity. However, there are no growth rules, which restrain the growing tiling from running into dead ends.

The eight different vertex configurations and their relative frequencies in the regular PT are shown in Fig. 1.7. The letter in the symbols indicates the topology, the upper index gives the number of linkages and the lower index the number of double arrows [16, 29].

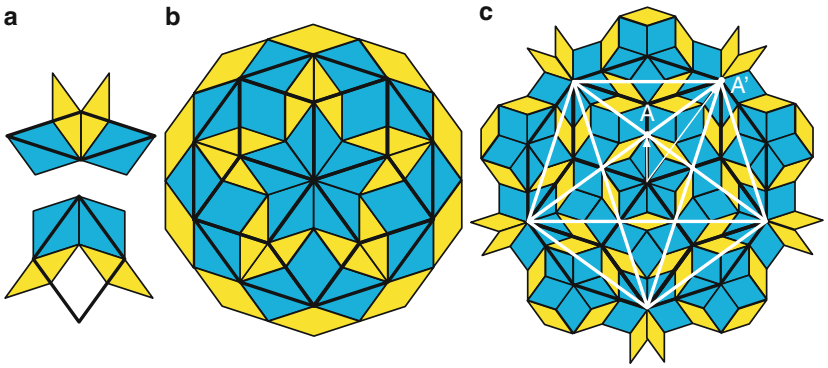

Fig. 1.6. Scaling properties of the Penrose tiling. (**a**) The substitution (inflation) rule for the rhomb prototiles. In (**b**) a PT (*thin lines*) is superposed by another PT (*thick lines*) scaled by S, in (**c**) scaling by S^2 is shown. A subset of the vertices of the scaled tilings are the vertices of the original tiling. The rotoscaling operation S^2 is also a symmetry operation of a pentagram (*white lines*), mapping each vertex of a pentagram onto another one. This is demonstrated in (**c**) on the example of the vertex A which is mapped onto A′ by S^2

The set of vertices of the PT, M_{PT}, is a subset of the vector module $M = \left\{\mathbf{r} = \sum_{i=0}^{4} n_i a_r \mathbf{e}_i \middle| \mathbf{e}_i = (\cos 2\pi i/5, \sin 2\pi i/5)\right\}$. M_{PT} consists of five subsets

$$M_{\mathrm{PT}} = \cup_{k=0}^{4} M_k \quad \text{with} \quad M_k = \left\{\pi^{\parallel}(\mathbf{r}_k) \middle| \pi^{\perp}(\mathbf{r}_k) \in T_{ik}, i = 0, \ldots, 4\right\} \tag{1.24}$$

and $\mathbf{r}_k = \sum_{j=0}^{4} \mathbf{d}_j \, (n_j + k/5)$, $n_j \in Z$ (for the definition of d_j see Sect. 3.1). The i-th triangular subdomain T_{ik} of the k-th pentagonal occupation domain corresponds to

$$T_{ik} = \left\{\mathbf{t} = x_i \mathbf{e}_i + x_{i+1}\mathbf{e}_{i+1} \middle| x_i \in [0, \lambda_k], x_{i+1} \in [0, \lambda_k - x_i]\right\} \tag{1.25}$$

with λ_k the radius of a pentagonally shaped occupation domain: $\lambda_0 = 0$, for $\lambda_{1,\cdots,4}$ see Eq. (3.138). Performing the scaling operation $\mathsf{S}M_{\mathrm{PT}}$ with the matrix

$$\mathsf{S} = \begin{pmatrix} 0 & 1 & 0 & \bar{1} \\ 0 & 1 & 1 & \bar{1} \\ \bar{1} & 1 & 1 & 0 \\ \bar{1} & 0 & 1 & 0 \end{pmatrix}_D = \left(\begin{array}{cc|cc} \tau & 0 & 0 & 0 \\ 0 & \tau & 0 & 0 \\ \hline 0 & 0 & -\frac{1}{\tau} & 0 \\ 0 & 0 & 0 & -\frac{1}{\tau} \end{array}\right)_V = \left(\begin{array}{c|c} \mathsf{S}^{\parallel} & 0 \\ \hline 0 & \mathsf{S}^{\perp} \end{array}\right)_V \tag{1.26}$$

yields a tiling dual to the original PT, enlarged by a factor τ. The subscript D refers to the 4D crystallographic basis (D-basis), while subscript V indicates that the vector components refer to a Cartesian coordinate system (V-basis) (see Sect. 3.1). Here S is applied to the projected 4D crystallographic basis (D-basis), i.e. the star of four rationally independent basis

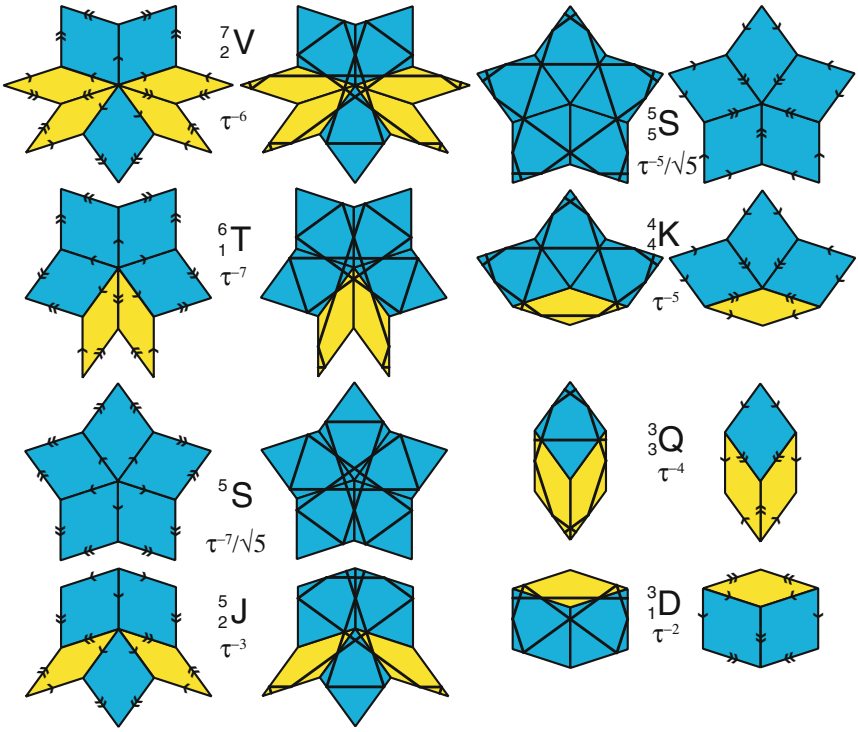

Fig. 1.7. The eight different vertex configurations of the regular Penrose tiling shown for decorations by *arrows* (*single* and *double*) and by Ammann line segments. The relative vertex frequencies are given below the vertex symbols. The configurations $^{5}_{5}$S, $^{4}_{4}$K, and $^{3}_{3}$Q transform into star (S), boat (B), and hexagon (H) tiles of the HBS tiling if those vertices are omitted where only double-arrowed edges meet (see Sect. 1.2.3.2)

vectors $\mathbf{a}_i = a_r \mathbf{e}_i,\ i = 1, \ldots, 4$. If a 2D Cartesian coordinate system is used, then the submatrix $\mathsf{S}^{\parallel}$ has to be applied.

Only scaling by S^{4n} results in a PT (increased by a factor τ^{4n}) of original orientation. Then the relationship $\mathsf{S}^{4n} M_{\mathrm{PT}} = \tau^{4n} M_{\mathrm{PT}}$ holds. S^2 maps the vertices of an inverted and by a factor τ^2 enlarged PT upon the vertices of the original PT. This operation corresponds to a hyperbolic rotation in superspace [20]. The rotoscaling operation $\Gamma(10)\mathsf{S}^2$ leaves the subset of vertices of a PT forming a pentagram invariant (Fig. 1.6).

By a particular decoration of the unit tiles with line segments, infinite lines (Ammann lines) are created forming a Fibonacci penta-grid (5-grid, "Ammann quasilattice" [23]) (Fig. 1.8). The line segments can act as matching rules forcing strict quasiperiodicity. In case of simpleton flips, the Ammann lines are broken (see Fig. 1.8). The dual of the Ammann quasilattice is the deflation of the original PT.

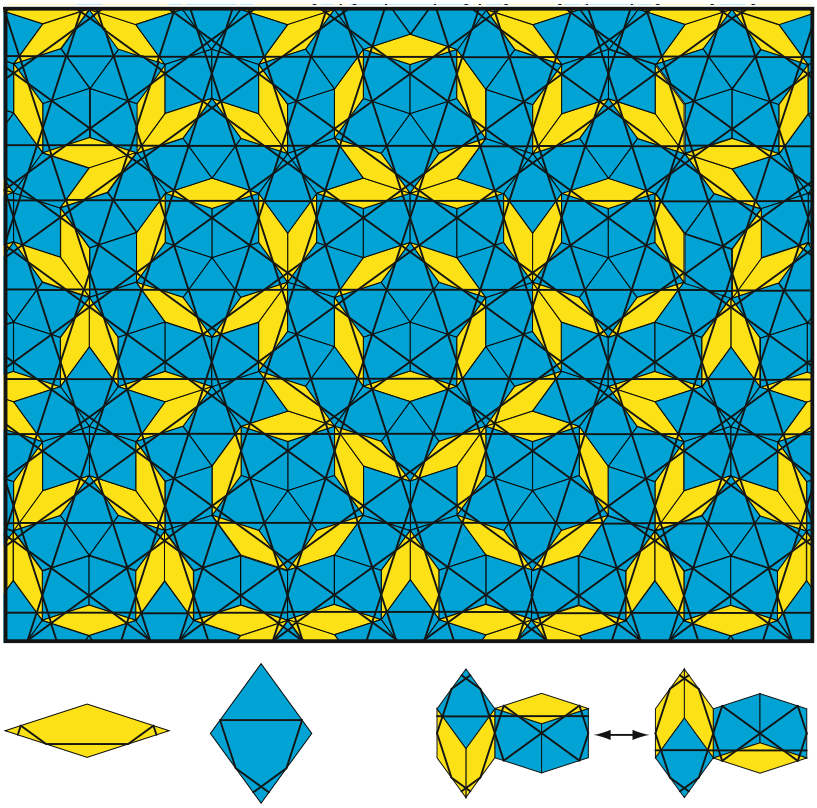

Fig. 1.8. The Penrose tiling with Amman lines drawn in. The decoration of the unit tiles by Ammann line segments and the action of simpleton flips are shown at the *bottom*

The third variant of the PT is the kite and dart tiling, denoted P2 tiling in the book by Grünbaum and Shephard [9]. Its relationship to the rhomb PT (P3) tiling is shown in Fig. 1.9. Starting with the kite and dart tiling (Fig. 1.9(a)), we cut the tiles into large acute and small obtuse isosceles triangles as shown in Fig. 1.9(b) and obtain the Robinson triangle tiling. The edge lengths of the triangles are in the ratio τ. While the black dots form a sufficient matching rule for the kites and darts, the isosceles triangles need, additionally, an orientation marker along the edges marked by two filled circles. In case of the acute triangle, this is an arrow pointing away from the corner where the isosceles edges meet; in case of the obtuse triangle, it is just the opposite.

If we fuse now all pairs of baseline connected acute triangles to skinny rhombs, and pairs of long-edge connected acute triangles together with pairs of short-edge linked obtuse triangles to fat rhombs, then we end up with a rhomb PT (Fig. 1.9(c)). The rhomb edge from the marked to the unmarked vertex also gets an orientation, which is usually marked by a double arrow.